LIMNOLOGY
and
OCEANOGRAPHY: METHODS

*Limnol. Oceanogr.: Methods* 7, 2009, 185–195

# A simple technique for continuous measurement of time-variable gas transfer in surface waters

*Craig R. Tobias,* John Karl Böhlke, Judson W. Harvey, Eurybiades Busenberg*
U.S. Geological Survey, Reston, VA, USA

## Abstract

Mass balance models of dissolved gases in streams, lakes, and rivers serve as the basis for estimating whole-ecosystem rates for various biogeochemical processes. Rates of gas exchange between water and the atmosphere are important and error-prone components of these models. Here we present a simple and efficient modification of the $SF_6$ gas tracer approach that can be used concurrently while collecting other dissolved gas samples for dissolved gas mass balance studies in streams. It consists of continuously metering $SF_6$-saturated water directly into the stream at a low rate of flow. This approach has advantages over pulse injection of aqueous solutions or bubbling large amounts of $SF_6$ into the stream. By adding the $SF_6$ as a saturated solution, we minimize the possibility that other dissolved gas measurements are affected by sparging and/or bubble injecta. Because the $SF_6$ is added continuously we have a record of changing gas transfer velocity (GTV) that is contemporaneous with the sampling of other nonconservative ambient dissolved gases. Over a single diel period, a 30% variation in GTV was observed in a second-order stream (Sugar Creek, Indiana, USA). The changing GTV could be attributed in part to changes in temperature and windspeed that occurred on hourly to diel timescales.

## Introduction

Determining the biogeochemical functions of streams, rivers, and estuaries at landscape scales is improved by techniques that provide whole-system estimates of transport and reaction rates. Often, these reach-scale approaches require measurements of biogenically derived gases (or gas ratios) and a subsequent accounting of sources and sinks of these gases to calculate the process rates of interest. Numerous examples of this approach exist, including $O_2$ metabolism (Odum 1956; Young and Huryn 1999; Mulholland et al. 2001), $N_2$ and $N_2O$ production via denitrification (McCutchan et al. 2003; Laursen and Seitzinger 2002, 2004), and carbon respiration (Cole and Caraco 1998). More recently, these gas mass balances have been coupled with stable isotopic measurements to improve resolution of the rate estimate (Böhlke et al 2004; Mulholland et al. 2004), simplify the solution of the gas mass balance (Quay et al. 1995; Russ et al. 2004), or provide additional insights into the underlying mechanisms controlling reaction rates (Bade and Cole 2006; Tobias et al. 2007). Several factors can confound interpretation of whole-system gas and/or isotopic mass balances, including groundwater fluxes, channel geometry, diel variability in reaction rates, and errors in estimating gas transfer velocity (GTV) (McCutchan et al. 2002; Böhlke et al.; 2004; Hall and Tank 2005; Laursen and Seitzinger 2005; McCutchan and Lewis 2006; Tobias et al. 2007). Impacts of these different factors vary between systems and become important in the final calculations when they are large components of the mass balance equations and when they exhibit high degrees of variability and/or uncertainty. Gas transfer exhibits both of these qualities. It can be a large flux term in the overall mass balance budget, particularly in shallow environments that have under- or oversaturated gas concentrations. GTV responds to changes in wind velocity (Wanninkhof et al. 1985; Liss and Merlivat 1986; Wanninkhof 1992) as well as to changes in temperature and channel turbulence (Bennett and Rathbun 1972; Young and Huryn 1999). Given the linear form of the equations governing the dissolved gas mass balances such as $O_2$ and $N_2$ (Mulholland et al. 2001; Laursen and Seitzinger 2002; McCutchan et al. 2003; Böhlke et al. 2004; Mulholland et al. 2004; Tobias et al. 2007),

---

*Corresponding author: E-mail: *tobiasc@uncw.edu
Current address: Department of Geography and Geology, UNC-Wilmington, Wilmington, NC 28403.

***Acknowledgments***

Stanley Mroczkowski, Karen Casciotti, Mary Voytek, Julie Kirshtein, Jessica Newlin, Joel Detty, Michael Doughten, and Peggy Widman contributed to this work. This study was supported by the USDA Cooperative State Research, Education, and Extension Service (National Research Initiative Competitive Grants Program in Watershed Processes and Water Resources) and by the USGS National Research Program in Water Resources, through the NRC postdoctoral fellowship program, and by NSF-DEB 0542635, NSF-EAR 0815201.

under- or overestimates of gas exchange translate proportionately into under- or overestimates of the biogenic gas production or consumption rate, respectively. Despite numerous site-specific estimates of gas exchange using conservative gas tracer additions, this term is still often regarded as one of the most error-prone terms in the open-channel calculations. All of the factors that impact gas transfer vary from hourly to monthly timescales.

Gas tracer experiments done for the purpose of estimating GTV usually involve the direct bubbling of large quantities of conservative gas (e.g., propane, $SF_6$) into surface waters. The bubbling may occur before or, in some cases, at least partially concurrent with the measurements of the biogenic gas of interest. Changes in the conservative gas concentration relative to a coadded solute tracer (e.g., $Br^-$ or $Cl^-$) or relative to a second gas tracer serve as the basis for the GTV calculation. Adding the gas tracer before sampling other ambient dissolved gases or gas ratios presumably avoids the effects of bubble injecta on those measurements, particularly at upstream locations nearest the input (Hibbs et al. 1998; Kilpatrick et al. 1989). It does not, however, provide a gas transfer estimate at the same time as the ambient biogenic gas measurements of interest, nor can it account for variation in GTV during the sampling period. Continuous bubbling of the conservative gas tracer concurrent with ambient biogenic gas monitoring alleviates this temporal disconnect, but it is inefficient (releasing large amounts of $SF_6$ to the atmosphere) and it does not address the potential for the gas sparging or bubble injecta to affect ambient gas, gas ratio, or gas isotope measurements. Improvements in open-channel dissolved gas budgets may be realized if time-varying GTV could be measured simultaneously with the measurements of ambient biogenic gases throughout the monitoring period.

Here we present a simple modification of the $SF_6$ gas tracer approach that can be used concurrently with collecting other dissolved gas samples used to calculate dissolved gas mass balances (e.g., $O_2$, $N_2$, $^{15}N_2$). It consists of continuously metering $SF_6$-saturated water into the stream. This type of gas tracer addition can be run continuously for several days and permits the GTV estimation on the same timescale as diel changes in biogenic gas concentrations. The approach was applied to a second-order stream and permitted observation of a 30% variation in GTV during a single diel period.

## Materials and methods

All field measurements occurred within a 1-km reach of Sugar Creek in western Indiana, USA (N 40°40′31″, W87°18′27″) in September 2003. Sugar Creek is a low-gradient, channelized stream with a streambed composed of coarse sand and fine gravel. This study was conducted during baseflow conditions ($Q \sim 18$ L s$^{-1}$) with a mean stream depth of 15 cm. Three sampling stations (upstream station A, midreach station B, and downstream station C) divided the 1-km stream reach into two subreaches (A–B and B–C).

*Tracer injection procedure*—As part of an ongoing isotopic and mass balance study investigating whole-stream $O_2$ metabolism and denitrification, gas transfer was estimated through the addition of two conservative tracers. One gas tracer ($SF_6$) and one solute tracer ($Br^-$) were added to Sugar Creek over a 32-h period. $SF_6$ and $Br^-$ were added simultaneously at the same location, but from separate reservoirs. The site of tracer injection was located 50 m upstream of the most upstream sampling station (A). Time series measurements of $SF_6$, $Br^-$, and the ambient gases of interest ($O_2$, $^{18}O_2$, $N_2$, $^{15}N_2$, and Ar) were made at all sampling stations.

$SF_6$ was introduced into the stream by a technique not typically used for releasing gas tracers in whole-stream studies. Rather than sparging gas tracer directly into stream water to achieve partial saturation, we added the $SF_6$ tracer at a much lower rate in the form of $SF_6$ saturated water. This approach had several advantages. It alleviated potential problems related to transient changes in $SF_6$ concentrations near the injection site caused by prolonged suspension of $SF_6$ microbubbles or potential gas stripping of ambient gases that might be caused by the sparging. The approach permitted us to measure gas transfer concurrently with the diel changes in the ambient gases of interest. Single slug additions of $SF_6$-saturated water to surface waters have been done previously for the purpose of estimating gas transfer (Hibbs et al. 1998; Upstill-Goddard et al. 1990). This type of single pulse, however, does not provide time-variable gas transfer information. Prolonged additions of $SF_6$ saturated water have been done previously to trace groundwater flowpaths (Gamlin et al. 2001), but not for the purpose of estimating air-water gas transfer in streams. Addition of propane-saturated water into streams has been tested (Jin et al. 2007), but propane analysis possesses a smaller analytical dynamic range than $SF_6$ and may deviate from conservative behavior during long addition durations.

The $SF_6$ tracer was prepared in a 40-L Tedlar (SKC Inc.) plastic sample bag that was floated in a tub of stream water (Figure 1). First, the bag was filled approximately halfway by pumping in 20 L of 1.0-μm-filtered streamwater with a peristaltic pump, and the remaining air headspace was allowed to escape through a port at the top of the bag until no air headspace remained. Then the headspace was refilled with approximately 10 L pure $SF_6$ that was transferred to the bag from a pressurized tank. The mixture was agitated repeatedly and allowed to equilibrate for approximately 24 h before the tracer experiment began, thereby creating a solution nearly saturated with $SF_6$ at 1 atm pressure. The outlet of the bag was weighted down to prevent accidental release of headspace gas to the pump during the experiment, and the $SF_6$-saturated (~0.25–0.30 mmol L$^{-1}$) tracer solution was pumped through Norprene tubing into the stream at a constant rate of 10 mL min$^{-1}$. Stream discharge at the injection site was 18.2 L s$^{-1}$, yielding a tracer:stream mixing ratio ($Q_{injectate}/Q_{stream}$) of approximately $9.2 \times 10^{-6}$ and a target initial stream $SF_6$ concentration of approximately 2.3–2.8 nmol L$^{-1}$ at the point of release.

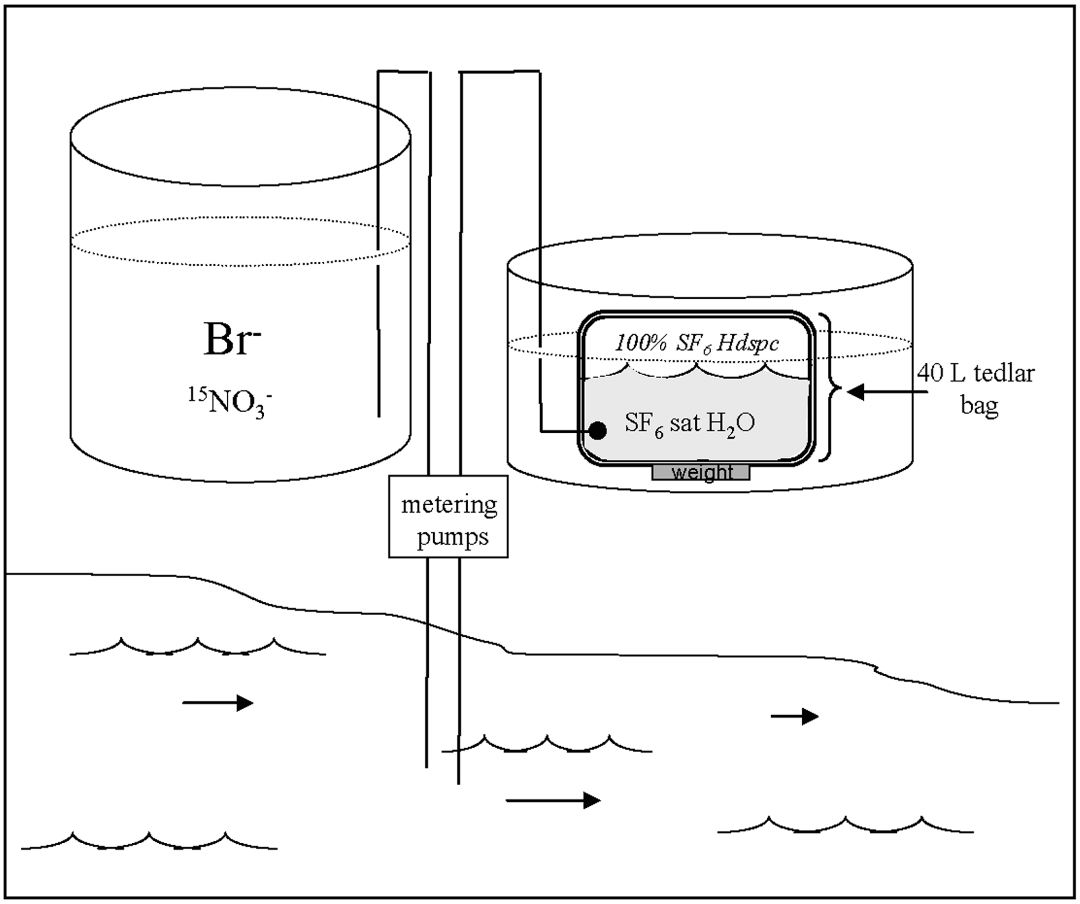

**Fig. 1.** Tracer injection design. Bromide and $SF_6$ tracer reservoirs were separated in this case to satisfy specific analytical requirements with low pumping rates, but this should not be necessary in other situations.

For the $Br^-$ solute tracer, NaBr was dissolved in stream water in a plastic barrel to give a $Br^-$ tracer concentration of 162 g $L^{-1}$. The $Br^-$ solution was pumped into the stream at a constant rate of 84 mL $min^{-1}$. The mixing ratio of the $Br^-$ tracer ($Q_{injectate}/Q_{stream}$) was approximately $7.5 \times 10^{-5}$, yielding a target initial $Br^-$ concentration in the stream of roughly 150 µmol $L^{-1}$.

Both the $SF_6$ and $Br^-$ tracer injections were pumped into the stream concurrently at middepth using metering pumps (FMI Inc.) operating continuously for 32 h. The injection site was located just upstream from a short reach containing riffles that facilitated mixing of tracer solution and streamwater before the first monitoring station. In our experiment, the $Br^-$ and $SF_6$ were prepared in different reservoirs because of the requisite differential pumping rates dictated by stream discharge and convenience for analytical methods. In other situations, however, it should be possible to combine $Br^-$ and $SF_6$ using this technique with appropriate adjustment of tracer concentrations and pumping rates for given stream flow and analytical limitations.

*Sampling and analysis*—Samples for $SF_6$ analysis were collected at the downstream monitoring stations (A, B, C) at 1- to 3-h intervals in pre-weighed 160-mL serum bottles that were capped with 12-mm-thick butyl rubber stoppers and preflushed with pure $N_2$. Approximately 10–20 mL water from the stream was injected into each bottle with a syringe. In the laboratory, the bottles were reweighed to determine the amount of sample, and the headspace was expanded into a 0.3016-$cm^3$ closed loop, then released through an Ascarite/$Mg(ClO_4)_2$ drier to a gas chromatograph with an electron capture detector (Busenberg and Plummer 2000; http://water.usgs.gov/lab/sf6/). The standard gas used for calibration had a $SF_6$ mole fraction of $1.499 \times 10^{-9}$. Headspace mole fractions were converted to aqueous concentrations based on sample and headspace volumes, temperature, and the measured internal pressure of the serum bottle. The detection limit for headspace $SF_6$ was 1.2 pptv. Analytical precision was 1.4% relative SD at 500 pmol $L^{-1}$. Overall uncertainties of $SF_6$ analyses were estimated to be 5%, including potential uncertainties in bottle weights, bottle pressures, calibration curves, and gas chromatography (GC) noise. The detection limit and operating range of the analysis can be much lower for other collection procedures, and the GC system is routinely used to measure background $SF_6$ concentrations with aqueous concentrations <2.0 fmol $L^{-1}$.

$Br^-$ samples were collected at each sampling station at 10-min intervals during tracer arrival and hourly after $Br^-$ plateau concentrations were reached. All of the samples were analyzed on a Dionex DX-120 with a Dionex AS-14 analytical column, AG-14 guard column, conductivity detector, 50-µL sample loop, and 3.5 mM sodium carbonate/1 mM sodium bicarbonate eluent. The $Br^-$ detection limit was 0.6 µmol $L^{-1}$.

Stream temperatures at all three sampling stations were recorded at 10-min intervals with HydroLab data sondes. Windspeed data were not available at the stream site, but were recorded at 30-min intervals at West Lafayette, Indiana, located ~40 km SE of the site (http://agmetx.agry.purdue.edu/sc.index.html).

*Calculation of GTV*—The $SF_6$ GTV was calculated for the whole study reach (between stations A and C) as well as for the two subreaches (A–B and B–C) at multiple time points during the 32-h study period according to

$$\mathrm{GTV}_{t_i+\Delta t/2} = -\ln\left[\frac{SF_6 / Br^-_{\mathrm{upstream},t_i}}{SF_6 / Br^-_{\mathrm{downstream},t_i+\Delta t}}\right] \times \frac{Z}{\Delta t} \qquad [1]$$

where $\mathrm{GTV}_{t_i+\Delta t/2}$ is approximately equal to GTV at the time a modeled parcel of water was halfway between the beginning and end of the subreach, $Z$ is the average depth (meters), $\Delta t$ is the tracer travel time (h) between the upstream and downstream sampling stations at the ends of a given subreach, $SF_6 / Br^-_{\mathrm{upstream},t_i}$ is the stream $SF_6/Br^-$ concentration ratio at the upstream sampling station at any a given time ($t_i$), and $SF_6 / Br^-_{\mathrm{downstream},t_i+\Delta t}$ is the stream $SF_6/ Br^-$ concentration ratio at the downstream sampling station at the time when the water represented by the upstream sample should have passed the downstream station ($t_i + \Delta t$). The $SF_6 / Br^-_{\mathrm{downstream},t_i+\Delta t}$ was either directly measured at $t_i + \Delta t$ or determined from the linear interpolation of sampling points that bracket $t_i + \Delta t$. The $Br^-$ concentrations adjust for the effect of dilution by groundwater discharge in the reach. Travel times were determined by least-squares fitting the $Br^-$ breakthrough curve at each station using the OTIS (One-dimensional Transport and Storage) program (Runkel 1998). The temporal resolution of the calculated GTV values is limited by the travel times between sampling stations and could be improved by closer spacing between sampling.

The general approaches for estimating GTV described above have been used in numerous studies (e.g., Wanninkhof et al. 1990; Mulholland et al. 2001; Laursen and Seitzinger 2002; Hall and Tank 2003; Mulholland et al. 2004), but our application is different from most in that our method of $SF_6$ tracer injection allows for a continuous record of GTV and is compatible with contemporaneous high-precision measurements of other dissolved gases.

## Results

GTVs were calculated for 11 time points for each of the subreaches. Estimates of GTV were made for the two individual subreaches (bracketed by sampling stations A–B and B–C) and for the whole study reach (bracketed by sampling stations A–C). Travel times derived from the $Br^-$ tracer data for subreaches A–B, B–C, and A–C were 4.0, 6.67, and 10.67 h, respectively (Figure 2). Dilution factors attributed to groundwater discharge $(Br^-_{\mathrm{upstream},t_i} / Br^-_{\mathrm{downstream},t_i+\Delta t})^{-1}$ were relatively constant during the experiment at 0.84, 0.81, and 0.68 for subreaches A–B, B–C, and A–C, respectively. Based on the observed $Br^-$ dilution, total integrated groundwater discharge was 3.4 L $s^{-1}$ for subreach A–B and 5.1 L $s^{-1}$ for subreach B–C. $SF_6$ concentrations decreased downstream from as high as 1300 pmol $L^{-1}$ at the upstream sampling station (A) to less than 100 pmol $L^{-1}$ at the downstream station (C). Plateau concentrations of $SF_6$ were more variable in the downstream stations than plateau concentrations of $Br^-$. This variability was manifested as both an extended time interval before reaching plateau relative to that of $Br^-$ and as inflections in postplateau $SF_6$ concentrations relative to $Br^-$. The initial delayed increase in concentration at station A may be attributed to incomplete equilibration between the water and $SF_6$ headspace in the Tedlar bag before the start of the injection, or possibly to the initial presence of some unsaturated water in the injection tubing. The postplateau inflections may be attributed in part to changes in the solubility of the $SF_6$ in the Tedlar bag caused by diel variations in temperature. Assuming the water in the Tedlar bag followed a diel temperature variation like that of the stream, using $SF_6$ solubilities for freshwater from Bullister et al. (2002), we calculated that the aqueous $SF_6$ concentration in the Tedlar bag could have ranged from ~0.23 to 0.30 mmol $L^{-1}$ over the diel cycle. This potential 18% change in the $SF_6$ source concentration should have generated diel waves in the input $SF_6$ concentration, but these waves were only marginally detectable in the stream. Much less diel variation in $SF_6$ was measured at the nearest sampling point (A) relative to downstream stations, indicating a much more stable $SF_6$ input concentration than would be expected if the bag temperature varied as much as stream temperature and if the $SF_6$ reequilibrated rapidly. The diel changes in downstream $SF_6$ concentrations at stations B and C therefore could be attributed mainly to the effects of changing GTV in the stream. Furthermore, because GTV was calculated from upstream versus downstream $SF_6$ concentrations in a moving parcel of water, smoothly changing reservoir concentrations of $SF_6$ should not substantially affect the GTV estimate if travel times are incorporated properly in the calculations.

The calculated GTVs for $SF_6$ varied by 30% over a 32-h period (Figure 3). Similar variations in GTV were observed in the estimates for both subreaches and for the whole reach calculation. The peak GTV (~0.06 m $h^{-1}$) occurred in all reaches at the same time (around 1400 h). The two periods of minimum GTV (~0.035 – 0.045 m $h^{-1}$) also occurred simultaneously in all reaches (around 0200 h).

Values of GTV determined with Equation 1 reflect the influence of all factors affecting GTV (e.g., temperature, wind speed, turbulence). Changes in stream temperature (17 to 25°C) and windspeed (0 to 4 m $s^{-1}$ at West Lafayette), two factors that affect GTV similarly, covaried over the sampling period (Figure 3). The highest GTV was observed at midday, when temperature

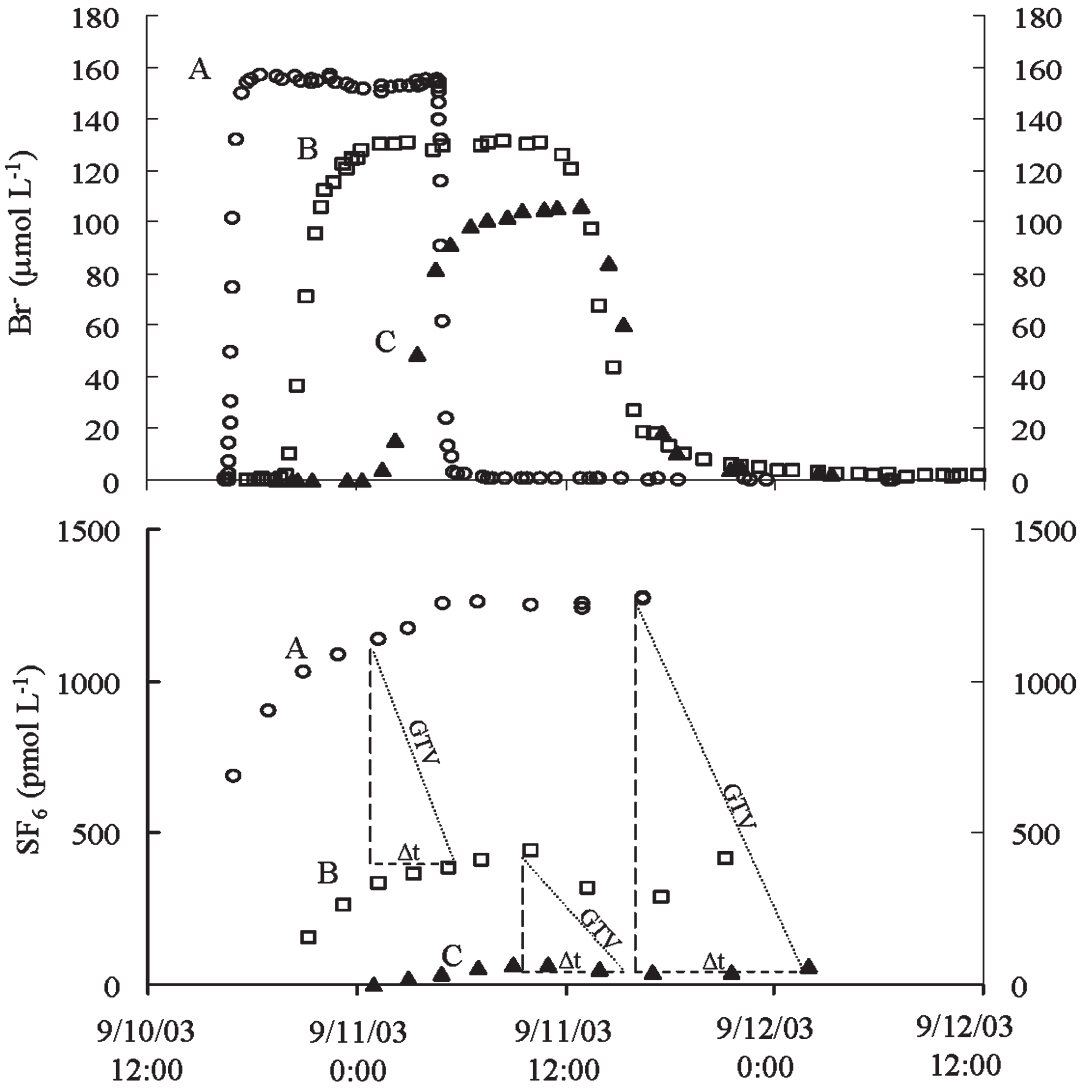

**Fig. 2.** Bromide tracer breakthrough curves and stream $SF_6$ concentrations. Diagonal lines connect measured $SF_6$ concentrations at different sampling stations adjusted for travel time. Travel time ($\Delta t$) used in the GTV calculations is shown as the horizontal component of the lines connecting sampling stations. $Br^-$ and $SF_6$ were pumped from separate reservoirs. The $Br^-$ addition ended before the $SF_6$ addition. Upstream–downstream $Br^-$ dilution factors calculated from plateau values were applied for all time intervals.

and windspeed were both at a maximum. Low GTV was observed at night, when temperatures and windspeed were both low. The minimum GTV was not, however, exactly coincident with the lowest windspeed or lowest temperature.

To examine the relative influence of temperature and windspeed on the observed temporal fluctuations in GTV, the GTV values measured using Equation 1 were normalized to temperature of 20°C ($GTV_{20}$) using the temperature correction equation presented in Thomann and Mueller 1987:

$$GTV_{20} = \frac{GTV}{1.024^{(T-20)}} \qquad [2]$$

where $T$ is stream temperature, GTV is calculated from Equation 1, and $GTV_{20}$ is the temperature-normalized gas transfer velocity. Significant linear correlations ($P < 0.001$) were observed between windspeed and gas transfer velocities that were both uncorrected (GTV) and normalized for temperature ($GTV_{20}$; Figure 4). Windspeed and temperature accounted for 44% (GTV; $R^2 = 0.44$) of the variance in observed in GTV. When gas transfer was normalized to temperature ($GTV_{20}$), thereby removing the covariance effect of wind and temperature on gas transfer, the correlation coefficient between windspeed and $GTV_{20}$ dropped to $R^2 = 0.29$. The temperature controls appeared most prominent in the early parts of the diel record, when variations in windspeed were smaller than those experienced in the last 16 h of the monitoring period.

## Discussion

*Potential advantages of continuous gas-saturated aqueous tracer additions*—The continuous addition of $SF_6$ to Sugar Creek at a

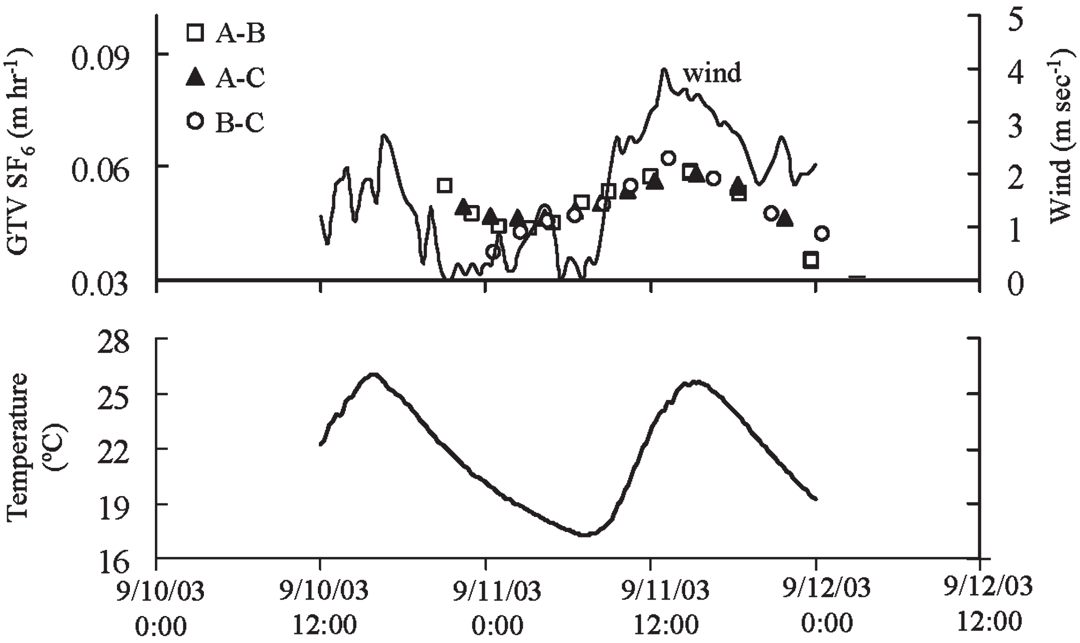

**Fig. 3.** Temporal variations in stream temperature, windspeed, and SF$_6$ gas transfer velocity (GTV). Temperature data are from Hydrolab sondes deployed in Sugar Creek; windspeed data are from West Lafayette, IN (~40 km SE of the site) (http://agmetx.agry.purdue.edu/sc.index.html); GTV values were determined from SF$_6$ tracer results for parcels that traversed the reach at specific intervals (plotted at the time when the parcel was midway through the reach). The highest GTVs were calculated when stream temperature and/or windspeed were highest. Close agreement was observed among GTV estimates calculated using subreach measurements (A–B and B–C) and whole-reach measurements (A–C).

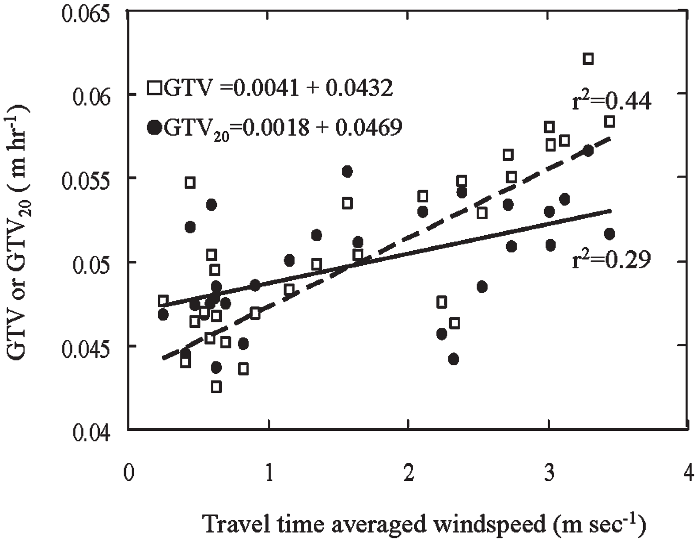

**Fig. 4.** Relations between windspeed and calculated GTV (open squares, $R^2$ = 0.44) and temperature-normalized gas transfer velocity (GTV$_{20}$; filled circles, $R^2$ = 0.29). Both correlations are significant at $P < 0.001$. Windspeeds correspond to the average windspeed recorded over the travel time for which the GTV was calculated. All GTV estimates calculated for the whole study reach and for each of the subreaches were used in the correlations.

low pump rate as a saturated aqueous solution had two major advantages not realized in many past gas tracer studies. It provided a continuous record of changing GTV for the length of the biogeochemical diel cycles being investigated, and because it avoided direct large-volume bubbling, it precluded gas stripping or bubble entrainment that might affect high-precision measurements of ambient dissolved gas concentrations. It also uses SF$_6$ efficiently, as it requires essentially no excess SF$_6$ beyond what mixes with the stream water and is measured in the stream. The ability to measure GTV continuously in real time could be useful in many types of open-channel gas calculations, particularly those in shallow and turbulent systems where atmospheric exchange is a large component of the gas budget. For example, determinations of whole-system denitrification rates rely on detecting small changes in N$_2$ concentration (Laursen and Seitzinger 2002, 2004; McCutchan et al. 2003) and/or N$_2$ isotopic composition in the case of isotope tracer studies (Böhlke et al. 2004, Mulholland et al. 2004), against large ambient N$_2$ inventories in surface water and air. The use of gas ratios (e.g., N$_2$/Ar) for this purpose can be susceptible to alteration from bubble injection and/or from bubble stripping. Dissolved gas stripping and alterations of dissolved gas compositions in waters subject to methane ebullition are well documented (e.g., Chanton et al.

1989). In the laboratory, denitrification rates based on membrane inlet mass spectrometry (MIMS) measurements of $N_2$/Ar ratios can be biased by the presence of bubbles that selectively incorporate $N_2$ relative to Ar, and similar potential difficulties could also affect field data. Balancing the need for direct GTV information with the preconditions for high-precision gas ratio measurements typically has required that gas tracer additions and ambient gas sampling be temporally decoupled (Laursen and Seitzinger 2002). Our technique should allow both continuous direct GTV and high-precision dissolved gas measurements to occur contemporaneously. We expect continuous GTV data will be most beneficial if incorporated into numerical simulations or inverse stepwise models that permit temporal and irregular variation of model parameters (e.g., Laursen and Seitzinger 2002; Böhlke et al. 2004; Tobias et al. 2007).

*Changing GTV in Sugar Creek*—The constant $SF_6$ addition allowed us to document a 30% variation in gas transfer during the diel monitoring period. The stable plateau concentrations of $Br^-$ measured at all stations (Figure 2) indicated that the diel inflections in $SF_6$ and hence GTV were not due to changes in stream hydraulic properties. Nor were the changes in GTV attributable to variations in the input concentration of the $SF_6$ saturated water, despite minor potential temperature-related changes in $SF_6$ solubility in the tracer reservoir.

Our results indicating changing GTV are qualitatively consistent with known affects of windspeed and temperature on gas transfer (Liss and Merlivat 1986; Wanninkhof 1992; Raymond and Cole 2001; Laursen and Seitzinger 2005). The observed correlations between the raw GTV and temperature normalized $GTV_{20}$ indicated that both temperature and windspeed contributed to the observed variation in gas transfer. The combined effects of temperature and windspeed accounted for 44% of the observed variance in GTV (Figure 4). Of that, approximately half could be attributed solely to temperature. Given the common practice of adjusting GTV for presumed temperature effects (e.g., Equation 2), it is important to be able to quantify deviations from this function. Other factors such as wind direction (which changed over the diel period) and stream channel orientation likely contributed to the additional variance in gas transfer. Stream turbulence may explain why GTV does not approach zero under no-wind conditions, in contrast to many empirical wind-versus-GTV relationships proposed for lakes and oceans. Although windspeed seems to have had an important effect on our GTV measurements, it is not possible to derive a meaningful predictive model of this effect from our data. First, although the timing of the wind variation recorded at the West Lafayette meteorologic station is consistent with qualitative observations made at the stream site during the experiment, the recorded data clearly cannot be considered to provide the precise timing or specific magnitude of wind at our site. Second, despite the significance of the correlations between windspeed and GTV, and $GTV_{20}$ observed here and by others (Laursen and Seitzinger 2005), there remain prominent outliers in the correlations that would lead to substantial error in deriving any given GTV estimate. The uncertainties of GTV values derived from the correlations presented for Sugar Creek (Figure 4) exceed a factor of 2 and are on par with uncertainties presented in other GTV–windspeed correlations across a wide range of sites (Raymond and Cole 2001; Laursen and Seitzinger 2005). The difficulty in generating precise GTV values from channel metrics, temperature, and windspeed that are reasonably transferable between sites, and on the same timescales of relevant biogeochemical reactions, underscores the benefit of a gas tracer approach that provides a continuous and direct measurement of GTV. Our approach should help to provide reduced uncertainty in diel GTV for any given study and contribute additional data for determining the applicability of proxy-derived estimates of GTV independent of gas tracer releases.

*Implications of changing GTV*—Because of the observed diel changes in GTV in Sugar Creek, any estimate based on measurements for a short time period within our diel time series had the potential to over- or underestimate GTV by as much as 30%. Moreover, because the observed variations in GTV were largely independent of stream flow and channel properties, measurements made on different days, or estimates derived from empirical relations with stream characteristics, could be incorrect by larger amounts. Laursen and Seitzinger (2005) report order-of-magnitude variation of GTV in Sugar Creek over a wider range of wind conditions. Uncertainty in GTV would be propagated in subsequent ambient gas mass balances and yield potential errors in estimates of biogeochemical rates of similar magnitude.

To illustrate implications of GTV variations like the ones we observed, we applied variable GTV scenarios to two types of in situ dissolved gas mass balances: (*1*) whole-stream metabolism based on diel $O_2$ measurements (Table 1) and (*2*) whole-stream denitrification estimates based on $^{15}NO_3^-$ tracer incorporation into dissolved $N_2$ gas (Figure 5). The metabolism scenarios are based on $O_2$ and $^{18}O_2$ measurements and mass balance models for Sugar Creek in 2003 as described in Tobias et al. (2007). The denitrification scenarios were derived from the $^{15}N$ and $N_2$ mass balance model for Sugar Creek in 2001 as described in Böhlke et al. (2004). For the metabolism and denitrification scenarios, we applied either time-varying GTV or constant GTV values that span the range of the diel GTV variation. The GTV for $SF_6$ was converted to GTV for $O_2$ or GTV for $N_2$ by multiplying by factors of 1.48 or 1.43, respectively.

For metabolism, we compared the effects of constant GTV set to minimum, maximum, or mean observed values to model results using variable GTV either directly measured or generated as a function of temperature (Table 1). The application of constant GTV for $O_2$ at either the minimum or maximum values caused both the calculated P (daily $O_2$ production) and R (daily $O_2$ reduction) values to differ proportionally (by a factor of 1.7) to the differences in GTV (Table 1), but P:R ratios remained relatively unchanged (Table 1). For the metabolism simulations

**Table 1.** Effects of uncertain and/or time variable gas transfer velocity (GTV) on $O_2$ metabolism in Sugar Creek. The constant GTV scenarios applied single values of GTV over the diel period corresponding to the minimum, maximum, and time-weighted mean of the measured GTV values. The temperature-variable GTV scenario used time-variable GTV calculated as a function of stream temperature according to a rearrangement of Equation 2 where $GTV_{20}$ was assigned a value (0.059) such that the time-weighted mean GTV for the diel period was equivalent to measured diel mean (0.060). The measured variable GTV scenario used direct measurements of GTV (Figure 3) over the diel metabolism period. P ($O_2$ production), R ($O_2$ reduction), and P:R ratios were derived for each GTV scenario from the $O_2$ and $^{18}O_2$ mass balance model for Sugar Creek presented in Tobias et al. (2007). P and R are reported as mmol $O_2$ $m^{-2}$ $h^{-1}$, averaged over a 24-h model period. GTV are reported for $O_2$ as m $h^{-1}$.

| GTV scenario | $O_2$ production (P) | $O_2$ reduction (R) | P:R |
|---|---|---|---|
| Constant $GTV_{\text{diel minimum}} = 0.050$ | 7.14 | 6.47 | 1.10 |
| Constant $GTV_{\text{diel maximum}} = 0.086$ | 12.33 | 10.90 | 1.13 |
| Constant $GTV_{\text{diel mean}} = 0.060$ | 8.90 | 8.00 | 1.11 |
| Temperature-variable $GTV_{\text{diel mean}} = 0.060$ | 9.09 | 7.64 | 1.19 |
| Measured variable $GTV_{\text{diel mean}} = 0.060$ | 11.70 | 9.60 | 1.22 |

using temperature-variable GTV, we rearranged Equation 2 to generate time-variable, temperature-dependent GTV values throughout the diel period. Although the temperature-variable GTV changed over time, the time-weighted diel mean was the same as that measured in the stream and used in the mean constant GTV scenario (0.060 m $h^{-1}$). Applying this temperature function to GTV showed that P and R were not equally affected, as observed in the constant GTV scenarios. The temperature function weighted GTV during the day when stream temperature was the warmest, when P was most active, and the greatest deviation from $O_2$ saturation was realized. Whereas P:R ratios changed little with different constant values of GTV, the

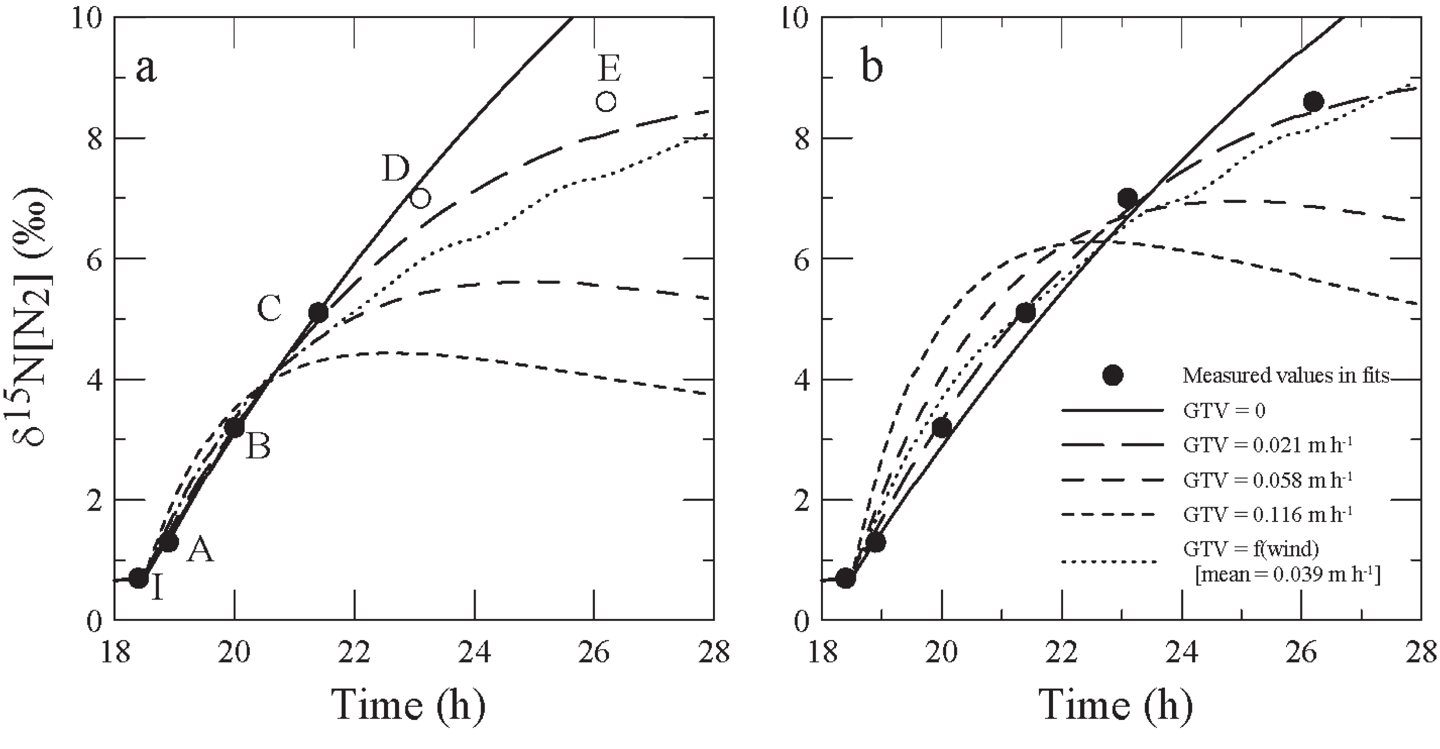

**Fig. 5.** The effects of changing GTV on in situ $^{15}N$-based stream denitrification models. Data and model are described in Böhlke et al. (2004). Data points A, B, C, D, and E denote sampling stations of increasing distance (and travel time) downstream. Model results were generated using denitrification rates that optimized model fit to the $\delta^{15}N_2$ data under the defined GTV scenarios in the figure (constant or wind-derived) and groundwater fluxes of $N_2$ specified in Böhlke et al. (2004). All fits were forced to go through $\delta^{15}N_2$ = 0.7 ‰ at time 0 (station I). (A) Models fit only to data from stations A, B, and C. Modeled denitrification rates were 85, 100, 89, 106, and 142 µmol $m^{-2}$ $h^{-1}$ for the GTV = 0.0, 0.021, 0.058, 0.116 m $h^{-1}$ and f(wind) scenarios, respectively. (B) Models fit to all stations. Modeled denitrification rates were 77, 112, 94, 136, and 214 µmol $m^{-2}$ $h^{-1}$ for the GTV = 0.0, 0.021, 0.058, 0.116 m $h^{-1}$ and f(wind) scenarios, respectively. Poor fits indicate unrealistic GTV scenarios, assuming denitrification was constant through the reach in each model.

variable GTV scenario yielded P:R ratios 10% higher than the constant GTV scenarios (Table 1). A larger increase in the P:R ratio was observed when the measured changes in GTV were applied to the metabolism model (Figure 3; Table 1). This higher P:R ratio compared to the temperature-derived GTV scenario is consistent with the observed covariance of wind with temperature during the day when P is active. These comparisons indicate that the timing of the changes in GTV (e.g., during the day when P is active versus at night when P is not) can impact estimates of net metabolism more than just incorrect estimates of constant GTV. Moreover, whereas windspeed and temperature were roughly correlated during our study (Figure 3), these variables commonly would vary independently, creating more complex temporal patterns of GTV variation.

For in situ denitrification studies using additions of $^{15}NO_3^-$ tracer, denitrification rates were derived from best model fits of $^{15}N_2$ enrichments measured at several stations downstream from the tracer input (Böhlke et al. 2004; Mulholland et al. 2004). Accumulation of $\delta^{15}N_2$ in these types of studies depends on the balance between the denitrification rate and GTV. Böhlke et al. (2004) tested various assumptions about GTV in simulations of downstream $^{15}N_2$ changes during a reach-scale $^{15}NO_3^-$ tracer experiment and showed that a good fit to the downstream $^{15}N_2$ enrichments was achieved through a time-variable GTV (in that case derived from windspeed, but not measured directly). New calculations were done here to evaluate sensitivity of results to uncertainty in GTV using the Böhlke et al. (2004) models and data. This analysis shows a moderate dependence of the model fit to GTV estimates for the early stages of $^{15}N_2$ enrichment (Figure 5A). For the Böhlke et al. (2004) data, the denitrification rates increased or decreased by approximately 50% to 60% of the respective changes in constant GTV. However, modeling the pattern of $^{15}N_2$ enrichment farther downstream, and especially the peak $\delta^{15}N_2$ enrichment (near-steady-state), proved highly sensitive to GTV, approaching the theoretical proportional changes in the calculated denitrification rate for a given change in GTV (Figure 5B). One result of this scenario testing is that denitrification model fits to multiple measurements from early stages of $^{15}N_2$ accumulation may actually provide constraints on permissible GTV (assuming denitrification is constant), whereas calculations from single points or plateau values are largely unconstrained in the absence of real-time GTV data.

These analyses of the potential implications of uncertain and/or time-variable GTV on in situ rate measurements illustrate two points. First, GTV measured on one particular day may, or may not, be directly applicable to ambient gas data collected on a subsequent day. Second, better estimates of time-variable GTV will yield better estimates of stream process rates. Because GTV and/or $GTV_{20}$ change on the same timescale (hourly) as biogeochemical rates of interest (e.g., photosynthesis, respiration, denitrification), continuous monitoring of GTV has the potential to improve quantification of diel variations in these processes and the underlying mechanisms that control them.

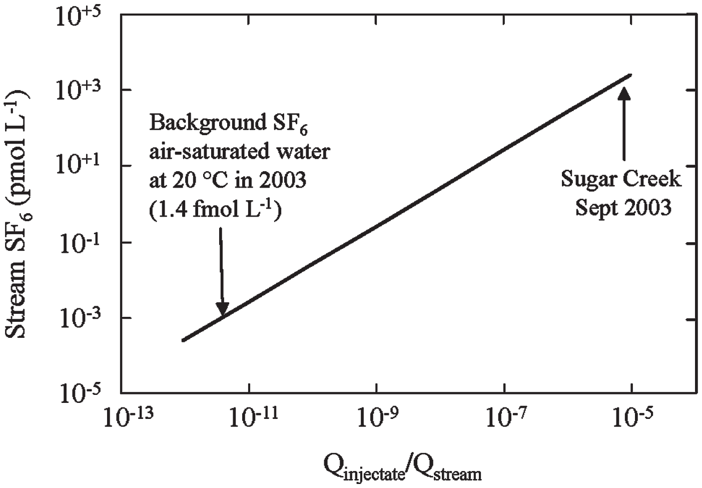

**Fig. 6.** Calculated stream $SF_6$ concentrations as a function of the unitless ratio of the injection rate of $SF_6$ saturated water ($Q_{injectate}$) to stream discharge ($Q_{stream}$). The pmol $L^{-1}$ concentration of $SF_6$ in the stream at the point of injection (following complete mixing) can be approximated using the equation: $SF_6 \approx 2.7 \times 10^8 \times [Q_{injectate}/(Q_{injectate} + Q_{stream})]$. This equation is based on the Henry's Law constant for $SF_6$ at 20°C, assumes a $SF_6$ partial pressure of 1.0 in the equilibration container (e.g., Tedlar bag), but in practice is subject to variation depending on temperature (Bullister et al. 2002). Additionally, the partial pressure of $SF_6$ in the headspace could be less than the local atmospheric pressure by as much as 5% because of $H_2O$ vapor and dissolved atmospheric gases released from the stream water into the headspace.

*Applications at larger scales*—This gas tracer study conducted on the scale of Sugar Creek relied on a slow pumping rate of $SF_6$-saturated water from a relatively small-volume collapsible reservoir (40L Tedlar Bag). Because the analytical detection limits for $SF_6$ are so low (Figure 6), the primary constraint on applying this approach to larger systems likely rests on achieving tractable pumping rates of the $SF_6$-saturated tracer and ensuring tracer-stream water mixing. Studies at larger spatial scales or for extended duration that require larger pumping rates, or longer pumping times, can be achieved by using a larger, gas-impermeable, collapsible reservoir such as an aircraft fuel bladder. These are commercially available in large volumes (>1000s of liters), can likely substitute for the Tedlar bag used in this study, and permit substantial increases in scale. For example, according to the relation in Figure 6, pumping $SF_6$-saturated tracer water at a rate of 144 $Ld^{-1}$ into a river with discharge of 50,000 cfs ($1.2 \times 10^{11}$ $Ld^{-1}$) yields an initial river $SF_6$ concentration that is two orders of magnitude above typical background concentrations ($SF_6 \approx 0.001$–$0.002$ pmol $L^{-1}$ in air-saturated water) and well above the analytical detection limit of $SF_6$ in water samples analyzed by GC-ECD (e.g., Busenberg and Plummer 2000). Adequate tracer mixing, however, would be a limiting factor in very large systems. Another practical consideration is that the $SF_6$-saturated water additions have the advantage of using less overall gas than direct sparging. A total of 10 L gas (at 1 atm) was used for our 32-h study. The general approach should also be useful for mixed gas tracer additions where a salt solute tracer is not used. Variants of our approach should prove applicable for direct measurement of gas exchange in larger systems and potentially address the need for improved measurements and modeling of biogeochemical cycling of dissolved gases in small to medium-sized rivers and in well-mixed estuaries (Raymond and Cole 2001).

## *References*

Bade, D. L., and J. L. Cole. 2006. Impact of chemically enhanced diffusion on dissolved inorganic carbon stable isotopes in a fertilized lake. J. Geophys. Res. 111, C01014, doi:10.1029/2004JC002684.

Bennett, J. P., and R. E. Rathbun. 1972. Reaeration in open-channel flow. US Geol. Survey Professional Paper #737, 75pp.

Böhlke, J. K., J. W. Harvey, and M. A. Voytek. 2004. Reach-scale isotope tracer experiment to quantify denitrification and related processes in a nitrate-rich stream, mid-continent United States. Limnol. Oceanogr. 49:821-838.

Bullister, J. L., D. P. Wisegarver, and F. A. Menzia. 2002. The solubility of sulfur hexafluoride in water and seawater. Deep-Sea Res. 49:175-187.

Busenberg, E., and L. N. Plummer. 2000. Dating young groundwater with sulfur hexafluoride: natural and anthropogenic sources of sulfur hexafluoride. Wat. Resour. Res. 36:3011-3030.

Chanton, J. P., C. S. Martens, and C. A. Kelley. 1989. Gas transport from methane-saturated, tidal freshwater wetland sediment. Limnol. Oceanogr. 34:807-819.

Cole, J. J., and N. F. Caraco. 1998. Atmospheric exchange of carbon dioxide in a low-wind oligotrophic lake measured by the addition of $SF_6$. Limnol. Oceanogr. 43:647-656.

Gamlin, J. D., J. F. Clark, G. Woodside, and R. Herndon. 2001. Large-scale tracing of ground water with sulfur hexafluoride. J. Env. Eng. 127:171-174.

Hall, R. O. Jr., and J. L. Tank. 2005. Correcting whole-stream estimates of metabolism for groundwater input. Limnol. Oceanogr. Methods 3:222-229.

——— and ———. 2003. Ecosystem metabolism controls nitrogen uptake in Grand Teton National Park, Wyoming. Limnol. Oceanogr. 48:1120-1128.

Hibbs, D. E., K. L. Parkhill, and J. S. Gulliver. 1998. Sulfur hexafluoride gas tracer studies in streams. J. Env. Eng. 124:752-760.

Jin, H., J. Ramsey, G. W. Kipphut, and D. S. White. 2007. Reaeration coefficient measurements using a modified propane injection method in western Kentucky streams. N. Am. J. Benthol. Soc., Annual Meeting Abstract 434.

Kilpatrick, F. A., R. E. Rathbun, N. Yotsukura, G. W. Parker, and L. L. DeLong. 1989. Determination of stream reaeration coefficients by use of tracers, book 3. Chap A18, Techniques of Water Resources Investigations of the U.S. Geological Survey, Denver, CO.

Laursen, A., and S. Seitzinger. 2005. Limitations to measuring riverine denitrification at the whole reach scale: effects of channel geometry, wind velocity, sampling interval, and temperature inputs of $N_2$-enriched groundwater. Hydrobiologia 545:225-236.

——— and ———. 2004. Diurnal patterns of denitrification, oxygen consumption and nitrous oxide production in rivers measured at the whole-reach scale. Freshwater Biol. 19:1448-1458.

——— and ———. 2002. Measurement of denitrification in rivers: an integrated, whole reach approach. Hydrobiologia 485:67-81.

Liss, P. S., and L. Merlivat. 1986. Air-sea gas exchange rates: introduction and synthesis. In: The role of air-sea exchange in geochemical cycling, P. Buat-Mènard (ed), p. 113-129. D. Reidel, Hingham, MA.

McCutchan, J. H. Jr., and W. M. Lewis. 2006. Groundwater flux and open-channel estimation of stream metabolism: Response to Hall and Tank. Limnol. Oceanogr. Methods 4:213-214.

McCutchan, J. H. Jr., J. F. Saunders III, A. L. Pribyl, and W. M. Lewis. 2003. Open-channel estimate of denitrification. Limnol. Oceanogr. Methods 1:74-81.

———, ———, W. M. Lewis Jr., and M. G. Hayden. 2002. Effects of groundwater flux on open-channel estimates of stream metabolism. Limnol. Oceanogr. 47:321-324.

Mulholland, P. J., H. M. Valett, J. R. Webster, L. W. Cooper, S. K. Hamilton, and B.J. Peterson. 2004. Stream denitrification and total nitrate uptake rates measured using a field 15N tracer addition approach. Limnol. Oceanogr. 49:809-820

——— and others. 2001. Inter-biome comparison of factors controlling stream metabolism. Freshwater Biol. 46:1503-1517.

Odum, H. T. 1956. Primary production in flowing waters. Limnol. Oceanogr. 1:102-117.

Quay, P. D., D. O. Wilbur, J. E. Richey, A. H. Devol, R. Benner, and B. R. Forsberg. 1995. The $^{18}O$:$^{16}O$ of dissolved oxygen in rivers and lakes in the Amazon Basin: determining the ratio of respiration to photosynthesis rates in freshwaters. Limnol. Oceanogr. 40:718-729.

Raymond, R. A., and J. J. Cole. 2001. Gas exchange in rivers and estuaries: choosing a gas transfer velocity. Estuaries 24:312-317.

Runkel, R. L. 1998. One-dimensional transport with inflow and storage (OTIS): a solute transport model for streams and rivers. U.S. Geological Survey Water Resources Investigation Report 98-4018.

Russ, M. E., N. E. Ostrom, H. Gandhi, P. H. Ostrom, and N. R. Urban. 2004. Temporal and spatial variations in R:P ratios in Lake Superior, an oligotrophic freshwater environment. J. Geophys. Res. 109:C10.

Thomann, R. V., and J. A. Mueller. 1987. Principles of surface water quality modeling and control. p. 282. Harper and Row.

Tobias, C. R., J. K. Böhlke, and J. W. Harvey. 2007. The oxygen-18 isotope approach for measuring aquatic metabolism in high-productivity waters. Limnol. Oceanogr. 52:1439-1453.

Upstill-Goddard, R. C., A. J. Watson, P. S. Liss, and M. I. Liddicoat. 1990. Gas transfer velocities in lakes measured with $SF_6$. Tellus 42B:364-377.

Wanninkhof, R., J. R. Ledwell, and W. S. Broecker. 1985. Gas exchange-wind speed relation measured with sulfur hexafluoride on a lake. Science 227:1224-1226.

———, P. J. Mulholland, and J. W. Elwood. 1990. Gas exchange rates for a first-order stream determined with deliberate and natural tracers. Wat. Resour. Res. 26:1621-1630.

———. 1992. Relationship between wind speed and gas exchange over the ocean. J. Geophys. Res. 97:7373-7382.

Young, R. G., and A. D. Huryn. 1999. Effects of land use on stream metabolism and organic matter turnover. Ecol. Appl. 9:1359:1376.

*Submitted 3 December 2008*
*Revised 15 January 2009*
*Accepted 1 February 2009*